



Development of an adaptive chemistry model considering micromixing effects

Ipsita Banerjee, Marianthi G. Ierapetritou*

Department of Chemical and Biochemical Engineering, Rutgers University, 98 Brett Road, Piscataway, NJ 08854-8058, USA

Received 1 April 2003; received in revised form 17 July 2003; accepted 22 July 2003

Abstract

In numerical simulation of combustion models, solution of the chemical kinetics is often the most expensive part of the calculation, since accurate description of kinetic mechanism involves large number of species and reactions, leading to a large set of coupled ODEs, often too complex to be considered in their entirety along with a detailed flow simulation. Hence the need for representing the complex chemical reactions by simple reduced models, which can retain considerable accuracy while rendering computational feasibility. Realistically, under different conditions and at different points in time, different reactions become important, which has been exploited to develop an *adaptive* reduction scheme such that the reduced reaction model adapts itself to the changing reactor conditions. A methodology is developed in this paper to construct reduced mechanisms by solving an optimization problem, where the objective is to determine the range of conditions along the reaction trajectory over which a prespecified number of reactions can predict the actual profile within an allowable tolerance. Such an adaptive reduced mechanism is then coupled with the reactive flow algorithm, which selects an appropriate mechanism depending on reactor condition and integrate the corresponding ODEs for the specified valid range. These ideas are demonstrated using the mechanism of CO/H₂ combustion in air.

© 2003 Elsevier Ltd. All rights reserved.

Keywords: Kinetic model reduction; Mixing; Mathematical modeling; Optimization

1. Introduction

The ability to predict the behavior of turbulent reacting flow is the most important factor in analysis of chemical reactors. In order to efficiently design and optimize such reactors, a reliable comprehensive model is needed that can accurately describe the turbulence-chemistry interactions. However, nonlinear chemical reaction rates introduce a severe closure problem for most practical turbulent flows modeled with moment methods (Cannon, Brewster, & Smoot, 1998). Pope (1985) derived a joint velocity-composition probability density function (PDF) from the conservation laws to describe the transport equations. This joint PDF provides complete statistical description of the random velocity and composition variables at each point in the flow field. It requires no modeling for convection, reaction and body forces and mean pressure gradient and hence overcomes

the chemical reaction rate closure problem associated with moment methods. Despite this exact chemical kinetic description, simplification in the reaction network is required to make the PDF method computationally tractable. For the last few decades there has been considerable effort towards alternative representation of detailed kinetic mechanisms to reduce the computational workload. One area of research is to represent the detailed kinetic model by a reduced reaction set, while retaining the desired model output, while another direction is to adaptively tabulate the species concentrations, which can be extracted during mixing simulation (Pope, 1997). Griffiths (1995) and Tomlin, Turanyi, and Pilling (1997) presents a comprehensive review of reduction techniques for kinetic models with emphasis on combustion. The techniques for mechanism reduction can be broadly divided into the following categories: (1) Quasi-steady state/partial equilibrium hypothesis (Peters & Williams, 1987; Lovas, Nilsson, & Mauss, 2000), (2) time-scale analysis (Mass & Pope, 1992; Lam & Goussis, 1994) and (3) mathematical programming methods (Petzold & Zu, 1997; Edwards, Edgar, & Manousiouthakis, 2000; Androulakis, 2000). In all

* Corresponding author. Tel.: +1-732-445-2971;
fax: +1-732-445-2421.

E-mail address: marianth@sol.rutgers.edu (M. G. Ierapetritou).

these techniques a simplified reactor model such as batch, plug flow or perfectly stirred tank is used to study the relative influence of individual reactions on the features of combustion processes. Transport effects are neglected while performing the reduction, but their influence is checked posteriori by testing full and reduced mechanisms in models that include these effects. However, it has been observed that the reduced mechanisms obtained thereby are valid over specific range of conditions and become considerably inaccurate when applied to conditions outside their range of validity (Sirdeshpande, Ierapetritou, & Androulakis, 2001). Moreover, the range of conditions encountered under turbulent reacting conditions can deviate significantly from the conditions simulated under the assumption of perfect mixing. Hence it is likely that a reduced mechanism valid under Perfectly Stirred Reactor (PSR) conditions will not retain its accuracy over the entire flow simulation.

To retain the desired accuracy over the entire flow simulation one always needs to use reaction mechanisms which are valid under current reactor conditions. Hence what is needed is different reduced reaction sets valid under different range of conditions, which will be selected appropriately during the simulation. In the present work an overall framework is presented for the adaptive reduction of complex kinetic networks and the integration with realistic mixing simulations. The performance of this reduction scheme is then analyzed under different mixing conditions.

In the next section the reduction technique adopted for this work is presented, followed by a description of the mixing model used for the reactor simulation and analysis of performance of reduced mechanism in mixing simulation in Sections 3 and 4. The adaptive reduction technique is then described in Section 5, followed by an algorithm to integrate it with the mixing simulation in Section 6. Finally, a detailed discussion of the various issues demanding further attention is presented in Section 7.

2. Mechanism reduction

The reduction technique adopted in this work follows the mathematical programming approach proposed by Androulakis (2000). This approach is based on determining the reactions of the detailed mechanism which can be excluded while still retaining a desired accuracy in the prediction of the profiles of certain important species. The reduction process begins with the choice of a reactor model and a discrepancy function, which is a measure of the error incurred in excluding reactions from the mechanism. The optimization problem for an isobaric batch reactor can be formulated as

$$\min_{\lambda \in A^{N_R}} \sum_{r=1}^{N_R} \lambda_r$$

subject to $\chi \leq \delta$,

(1)

$$\text{where, } \chi = \left(\sum_{k \in \kappa} \int_{t_i}^{t_f} \left(\frac{y_k^{\text{reduced}}(t) - y_k^{\text{full}}(t)}{y_k^{\text{full}}(t)} \right)^2 dt + \int_{t_i}^{t_f} \left(\frac{T_k^{\text{reduced}}(t) - T_k^{\text{full}}(t)}{T_k^{\text{full}}(t)} \right)^2 dt \right)^{1/2}, \quad (2)$$

$$\frac{dy_k(t)}{dt} = \frac{R_k M_k}{\rho} \quad k = 1, \dots, N_s, \quad (3)$$

$$\frac{dT}{dt} = - \sum_{k=1}^{N_s} \frac{R_k M_k h_k}{\rho \bar{C}_p}, \quad (4)$$

$$R_k = \sum_{i=1}^{N_r} \lambda_i (v_{k_i}^r - v_{k_i}^f) q_i, \quad (5)$$

$$q_i = k_{f_i} \prod_{k=1}^{N_s} X_k^{v_{k_i}^f} - k_{r_i} \prod_{k=1}^{N_s} X_k^{v_{k_i}^r}, \quad (6)$$

$$k_{f_i} = K_{f_i} e^{-E_{f_i}/RT}, \quad k_{r_i} = K_{r_i} e^{-E_{r_i}/RT}, \quad (7)$$

where, λ_r is a binary variable used to denote the presence ($\lambda_r = 1$) or absence ($\lambda_r = 0$) of a particular reaction. Hence, the objective function $\sum_{r=1}^{N_R} \lambda_r$ represents the total number of reactions in the reduced set, which has to be minimized, subject to a specified accuracy (δ). The integral error measure χ , given by Eq. (2), defines the approximation error of the trajectories of the key observable quantities for the interval of interest. In the above formulation, y_k denotes the mass fraction whereas X_k represents the molar concentration of species k used in the calculation of the reaction rates. Eqs. (3) and (4) represent the material and energy balance for the reactor model, where R_k is the net rate of production of species k ; M_k is the molecular weight of species k ; ρ denotes the mixture density, which is a function of composition and temperature. R_k is evaluated from the knowledge of intrinsic rates q_i of individual reactions and stoichiometry, as given by Eq. (5). For combustion systems, the basic form of q_i is expressed by the power law expression of mass-action kinetics, as given by Eq. (6). The temperature dependence of the specific reaction rate constant is given by Arrhenius law (Eq. (7)).

Formulation (1)–(7) of mechanism reduction correspond to an integer nonlinear programming problem which can be solved using a Branch and Bound framework (Androulakis, 2000). The solution procedure can be greatly enhanced by a priori determination of a subset of important reactions, thereby reducing the total number of binary variables considered in the Branch and Bound framework. The approach adopted to determine a critical set of reactions ($N_{R_{\min}}$) that cannot be removed from the mechanism is as follows: if eliminating reaction i from the detailed network ($\lambda_i = 0$) while retaining all other reactions ($\lambda_j = 1, j = 1, \dots, N_R, j \neq i$) produces a reduced network with $N_r' = N_R - 1$ reactions that approximates the complete network with an error $\delta' > \delta$, then reaction i must be retained in the reduced set and need not be treated as a variable in the optimization problem.

Hence, the optimization is now constrained on the remaining $N_R - N_{R\min}$ reactions, from which the minimum number of reactions needs to be identified. However, compensating errors can be present, whereby removing reaction *A* or reaction *B* can result in an error, but removing reactions *A* and *B* together might cancel out individual errors. Such compensating errors cannot be identified by the heuristics. Hence, when such a preprocessing step is employed, the final reduced reaction set obtained might not be optimal.

In the present work, Genetic Algorithm (GA) has been used as the solution procedure for the mechanism reduction problem, following the work of Edwards, Edgar, and Manousiouthakis (1998). GA (Goldberg, 1989; Michalewicz & Schoenauer, 1996) represent a class of search and optimization procedures that are patterned after the biological process of natural selection and they lend themselves to solution of a wide range of optimization problems. When GA is applied to optimization problem, each optimization variable is typically encoded as a string of bits, and these strings are appended together to form a chromosome. Each individual in a population has a particular chromosome value that can be decoded to evaluate the parameter values and objective function, also called the fitness function. Populations are evolved through several generations until the objective function cannot be improved any further.

In the present formulation the optimization variables are the N_R binary variables associated with the reactions. Hence parameterisation for GA is straightforward since each binary variable λ_r becomes a bit in the GA chromosome. For a particular combination of λ_r , the reduced differential equation sets are integrated to evaluate the discrepancy function. Since GA cannot explicitly handle nonlinear constraints of an optimization problem, there has been considerable research towards efficient constraint handling while using GA. Most of the constraint handling methods are based on the concept of (exterior) penalty functions (Michalewicz & Schoenauer, 1996) that penalize the infeasible solution and try to solve an unconstrained problem using a modified fitness function. The unconstrained optimization formulation for problem (1)–(7) can be represented as

$$\min_{\lambda \in A^{N_R}} \sum_{r=1}^{N_R} \lambda_r + (\text{penalty} \times \max\{0, \chi - \delta\}), \quad (8)$$

where the penalty term becomes zero when the constraint is not violated ($\chi < \delta$), and it takes the value of a large positive quantity (penalty $\times (\chi - \delta)$) otherwise. Note that the penalty coefficient needs to be large enough to ensure that all the infeasible solutions have fitness value worse than any of the feasible solutions. Unlike classical search and optimization methods, GA approach begins its search with a random set of solutions, instead of just one solution.

For the solution of problem (1)–(7), the first step of the GA procedure involves the random generation of a large

population of binary strings (reaction combinations) where each member of the population represents a reduced reaction set. For each reduced set within the initial population the corresponding ODEs are integrated to evaluate the discrepancy function and hence the fitness function, as given in Eq. (8). The integration is performed using LSODE (Hindmarsh, 1983) while the rate expressions and all the necessary thermodynamic properties are evaluated using the CHEMKIN-III package (Kee, Rupley, Meeks, & Miller, 1996). The generated population of solutions are modified by the GA operators (reproduction, crossover, mutation) to create new and better populations. This procedure is repeated until a predefined termination criteria is satisfied. There are several advantages of using GA for the mechanism reduction problem as compared to Branch and Bound procedure. First, the computation time of Branch and Bound depends highly on the quality of the initial reaction set produced within the preprocessing heuristic step, since the closer it is to the optimal solution the less number of nodes are required. However, as mentioned above, the method of generating the initial guess can prevent optimality of the solution. Since GA does not require such a reaction subset to start the solution procedure, this problem is avoided. Second, in the Branch and Bound procedure, at each node of the binary tree a nonlinear optimization problem needs to be solved, which requires information of the gradient of the constraint function, that corresponds to an expensive computational step. Moreover, since the NLP is in general nonconvex, no guarantee of the global optimal solution is possible. GA does not require gradient evaluation since the only information needed is the value of the discrepancy function for certain combinations of reaction sets. On the other hand however, the optimal solution obtained by using GA depends heavily on the termination criteria that are predetermined by the user, which can be a limitation. For the present studies, the simulation was allowed to run sufficient number of times until no significant change in the objective function was observed, which is however not sufficient to guarantee optimality of the obtained solution. In the present simulation using CO/H₂ mechanism, a population size of 10 was used for 200 iterations, which required CPU time of 310.9 s using Sun Solaris-8 that is used in all the computations reported in this paper. GA is adopted in this work since the target is to generate a number of reduced kinetic networks that will be used within the adaptive chemistry framework (Section 5), and not the determination of a single optimal reduced network.

The above formulation minimizes the total number of reactions involved in the kinetic source term, and the number of binary variables equals the total number of reactions. For a typical combustion system, the number of reactions far exceeds the total number of species. For example, methane combustion following GRI-3.0 mechanism involves 53 species and 325 reactions. For such a system a preprocessing step of species reduction was observed to be more efficient in solving the optimization problem. The formulation

of species reduction is given to be (Androulakis, 2000):

$$\min_{\lambda \in A^{N_s}} \sum_{i=1}^{N_s} \lambda_s$$

subject to $\chi \leq \delta$,

$$\chi = \left(\sum_{k \in \kappa} \int_{t_i}^{t_f} \left(\frac{y_k^{\text{reduced}}(t) - y_k^{\text{full}}(t)}{y_k^{\text{full}}(t)} \right)^2 dt + \int_{t_i}^{t_f} \left(\frac{T_k^{\text{reduced}}(t) - T_k^{\text{full}}(t)}{T_k^{\text{full}}(t)} \right)^2 dt \right)^{1/2},$$

$$\frac{dy_k(t)}{dt} = \frac{R_k M_k}{\rho} \quad k = 1, \dots, N_s,$$

$$\frac{dT}{dt} = - \sum_{k=1}^{N_s} \frac{R_k M_k h_k}{\rho \bar{C}_p},$$

$$R_k = \sum_{i=1}^{N_r} \prod_{s=1}^{N_s} (\lambda_s)_r (v_{k_i}^r - v_{k_i}^f) q_i,$$

$$(\lambda_s)_r = \begin{cases} \lambda_s & \text{if species } s \text{ participates in reaction } r, \\ 0 & \text{otherwise,} \end{cases} \quad (9)$$

where λ_s is a binary variable corresponding to each species. Elimination of species directly reduces the number of ODEs in the representation of source term. Hence, all the reactions in which those particular species participate, get eliminated. This results in a preliminary reduced reaction set, on which further reduction can be performed using the formulation consisting of Eqs. (1)–(7).

3. Reactor model

The reactor model assumed in order to develop the mathematical formulation (1)–(7) is the perfectly stirred reactor (PSR), which has been popularly used to study the chemistry of various batch chemical processes. The basic assumption underlying a PSR is that high-intensity turbulent mixing causes contents of the reactor to be completely mixed instantaneously. As a consequence of this perfectly mixed condition, the rate of chemical processes is controlled by chemical kinetic rates and not by the mixing process. While PSR can provide valuable insights into the nature of chemical kinetics, many practical applications deviate significantly from the ideally mixed situation. When the turbulent mixing rate is not fast compared to chemical kinetics, the degree of mixing can have a profound impact on the reactor characteristics. To assess the effects of the unmixed nature on various thermo-chemical properties inside the reactor, simulation of partially stirred reactor (PaSR) has been proposed (Correa, 1993).

3.1. Partially stirred reactor model

The salient feature of the PaSR model is the unmixed nature of the reactive fluids at the molecular level. Inside the

reactor, the mean thermo-chemical properties are assumed to be spatially homogeneous but imperfectly mixed at molecular level. That is, the reactive fluids are not completely diffused into each other at the molecular level, but their mean values are uniform throughout the reactor due to turbulent stirring. With the above assumption, Curl (1963) derived the probability density function (PDF) evolution equation for a single reactive scalar. To generalize this approach for multiple reactive scalars, the transport equation for the joint PDF is derived by integrating the governing equation for the single-point joint scalar PDF (Pope, 1985) over the reactor volume. The resulting PDF equation for the PaSR (Chen, 1997; Cannon et al., 1998) is given by :

$$\frac{\partial \tilde{P}_{\bar{\phi}}(\bar{\psi}, t)}{\partial t} = - \sum_{\alpha=1}^k \frac{\partial}{\partial \psi_{\alpha}} \{ S_{\alpha}(\bar{\psi}) \tilde{P}_{\bar{\phi}}(\bar{\psi}, t) \} + \frac{1}{\tau_{\text{res}}} \{ \tilde{P}_{\bar{\phi}, \text{inlet}}(\bar{\psi}) - \tilde{P}_{\bar{\phi}}(\bar{\psi}, t) \} - \sum_{\alpha=1, \beta=1}^k \frac{\partial^2}{\partial \psi_{\alpha} \partial \psi_{\beta}} \{ \langle \varepsilon_{\alpha\beta} | \bar{\phi} = \bar{\psi} \rangle \tilde{P}_{\bar{\phi}}(\bar{\psi}, t) \}, \quad (10)$$

where $\tilde{P}_{\bar{\phi}}(\bar{\psi}, t)$ is the density-weighted joint composition PDF; $\tilde{P}_{\bar{\phi}, \text{inlet}}$ is the composition PDF at the reactor inlet; $\bar{\psi}$ is the independent composition vector; $\bar{\phi}$ is the random composition vector whose PDF needs to be determined; $S_{\alpha}(\bar{\psi})$ is the instantaneous reaction rate for chemical species α ; τ_{res} is the average residence time in the reactor; $\varepsilon_{\alpha\beta}$ denotes the scalar dissipation rate; the term $\langle \varepsilon_{\alpha\beta} | \bar{\phi} = \bar{\psi} \rangle$ represents the expected value of $\varepsilon_{\alpha\beta}$ conditioned upon a particular event $\bar{\phi} = \bar{\psi}$. Fluctuating velocities are not considered and a constant mass flow is assumed. In Eq. (10) the first two terms on the right-hand side represent the effects of chemical reaction and the through-flow on the joint scalar PDF, respectively. Both these terms do not need modeling. The last term stands for the effect of microscale mixing on the PDF, which can be modeled using Interaction-by-Exchange-with-the-Mean (IEM) model (Dopazo, 1975) or Coalescence-Dispersion (CD) model (Curl, 1963). From general view of modeling turbulent reactive flow, PaSR can be considered as a single grid cell embedded in a large computational scheme. Therefore, PaSR offers an ideal test bed for exploring the influence of the unmixed nature on chemical kinetics, for evaluating the performances of reduced chemistry, and for assessing various mixing models and thus is adopted in this work.

3.2. Stochastic simulation of PaSR

A stochastic modeling approach for PaSR has been developed by Correa (1993) for premixed combustion and by Chen (1997) for nonpremixed combustion, where the PDF is represented by an ensemble of N_p particles, each having a unique composition. The PDF $P(Y_k)$ of mass fraction Y_k of

the species in the reactor is represented by the N_p ensemble:

$$Y_k^{(1)}, Y_k^{(2)}, \dots, Y_k^{(N_p)}, \quad k = 1, \dots, N_s. \quad (11)$$

A time marching scheme is used for the stochastic simulation which is carried out by the following sequential procedure:

1. Throughflow is simulated by randomly selecting fluid particles from the ensemble of N_p particles at the specified mass flow rate. The properties of these selected particles are set to the properties of the incoming mixture, and their age is reset to zero. The number of fluid particles to be replaced at each time step (Δt) (Borghini, 1988) is given by:

$$N_{\text{replaced}} = \frac{\Delta t}{\tau_{\text{res}}} N_p. \quad (12)$$
2. Fluid particles in the reactor are allowed to mix at the prescribed mixing frequency. This can be achieved by using one of the micromixing models, CD or IEM, as mentioned in the previous section.
3. The mixed fluid particles are now allowed to react according to chemical kinetic rate equations.

3.2.1. Modeling PaSR with IEM model

While using IEM to model molecular mixing, reaction and mixing are considered simultaneously, and fractional time stepping is not required. The governing equation for each particle is given by

$$\frac{dY_k^{(n)}}{dt} = -\omega(Y_k^{(n)} - \bar{Y}_k) + R_k^{(n)}M_k/\rho^{(n)},$$

$$k = 1, \dots, N_s; \quad n = 1, \dots, N_p, \quad (13)$$

where ω is the mixing frequency, $R_k^{(n)}$ is the molar production rate of species k per unit volume of the n th particle, M_k is the molecular weight of species k and $\rho^{(n)}$ is the density of the n th particle. The corresponding equation for the particle temperature is

$$C_p \frac{dT^{(n)}}{dt} = -\omega \sum_{k=1}^{N_s} Y_k^{(n)} (h_k^{(n)} - \bar{h}_k) + \sum_{k=1}^{N_s} h_k^{(n)} R_k^{(n)} M_k / \rho^{(n)}. \quad (14)$$

The first term on the right-hand side of Eq. (13) describes linear deterministic relaxation to the mean, which is the main characteristic of the IEM model. The second term is the reaction rate term for species k , which introduces significant complexity and stiffness.

For each of the N_p particles, Eq. (13) is solved for each of N_s species and Eq. (14) for temperature. The quantities required in the IEM model are updated from the ensemble. This procedure is repeated until a stochastic steady state is achieved. If, however, a large change occurs in the current particle (the one under integration), the mean quantities will be affected during the current time step and the IEM model term will be incorrect. This places a restriction on the maximum allowable change within the global time step, and hence a restriction on the maximum allowable time step.

PaSR simulation is performed with progressively smaller time steps until convergence of mean statistics is established.

3.2.2. Modeling PaSR with CD model

When modeling mixing by the CD model, the mixing and reaction steps has to be considered separately. To simulate the mixing step, N_{mix} pairs of particles are randomly chosen and are allowed to mix by averaging their scalar values, before returning them to the ensemble. The value of N_{mix} is given by Pope (1982):

$$N_{\text{mix}} = 2N_p \omega \Delta t. \quad (15)$$

To illustrate the case for a conserved scalar ζ , consider the mixing of one pair out of N_{mix} pairs of particles which are mixed at each time step. If the two particles have value ζ_1 and ζ_2 at the beginning of the time step, then according to Curl's model, their values at the end of the time step (Correa, 1995) will be given by:

$$\zeta_1^{\text{new}} = \zeta_2^{\text{new}} = \frac{1}{2}(\zeta_1 + \zeta_2). \quad (16)$$

Following mixing, the mass fractions and temperature of each particle in the ensemble are advanced in time by integration of the chemical kinetic equations.

4. Evaluation of reduced chemistry model

The reduced kinetic mechanism determined for perfect mixing conditions using model (1)–(7) is used in the PaSR model to evaluate its performance under finite mixing rates. Simulation was performed for CO/H₂ combustion in air (Li & Rabitz, 1997). The kinetic scheme consists of 47 reversible reactions, 14 species and is given in the appendix. The initial conditions considered are: H₂ mol frac. = 0.005, O₂ mol frac. = 0.189, CO mol frac. = 0.095, N₂ mol frac. = 0.711, $T_0 = 1600$ K, residence time = 8 ms. The observed species for the present simulation are CO, O₂, H₂, CO₂ and temperature. A 5-step reduced mechanism was obtained using PSR model, consisting of reactions {3, 6, 10, 17, 38}. Integration of this reduced mechanism using the PSR model required a CPU time of 0.05 s, as compared to CPU requirement of 0.16 s for the detailed mechanism, using Sun Solaris-8. It is also worth mentioning that although this 5-step reduced mechanism has similar number of species (11 compared to 14 in detailed mechanism), the reduction in CPU time is significant. Since reduction of the number of species directly reduces the number of ODEs to be integrated, it results in considerable savings in CPU time. However, reaction reduction will reduce the coupling of the ODEs, which also results in considerable computational savings. To illustrate this, another reduced mechanism is considered, consisting of 11 species and 26 reactions, which requires 0.11 s for the integration using PSR, as compared to 0.05 s required by the mechanism with 11 species and 5 reactions.

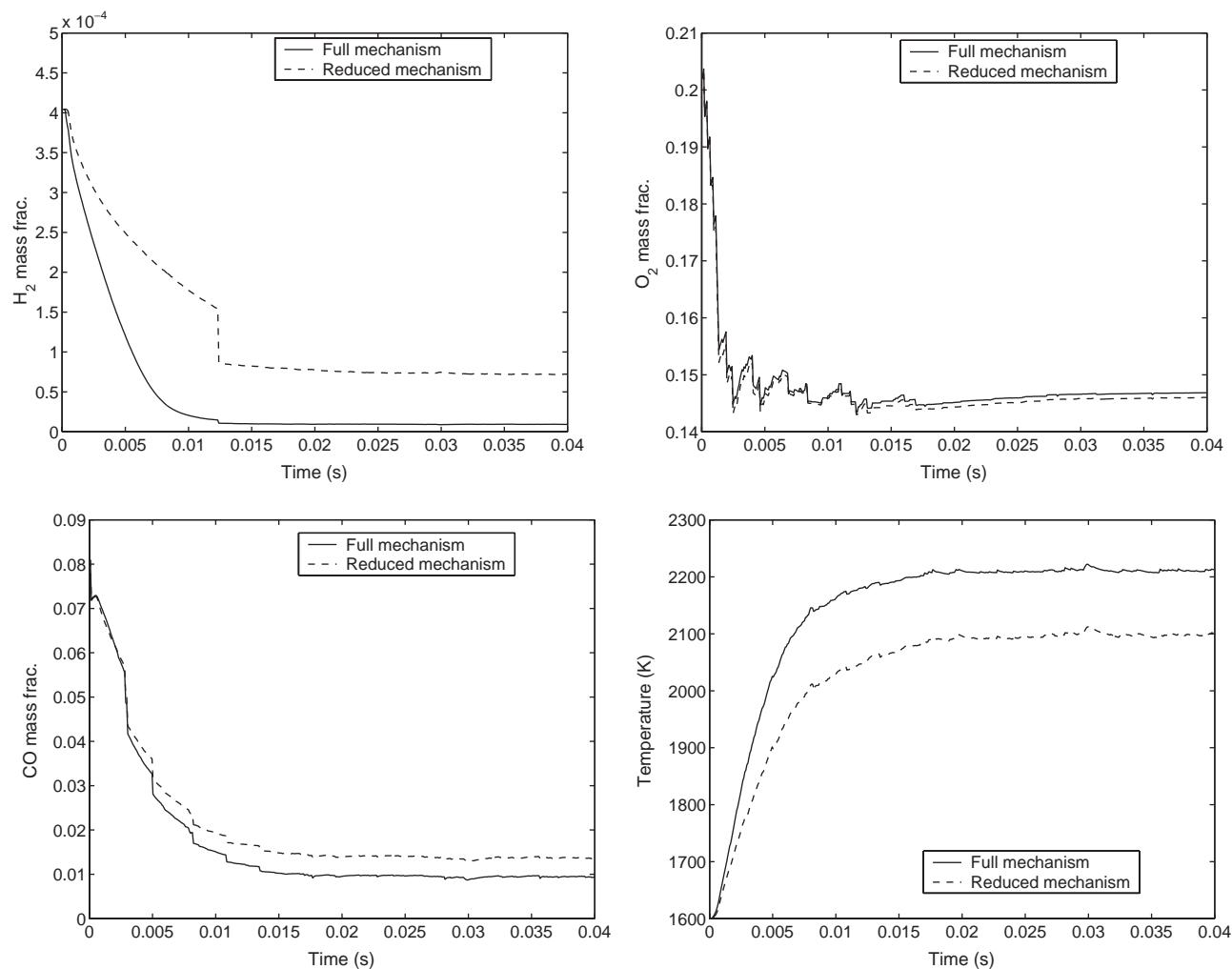


Fig. 1. Comparison between profiles of detailed and reduced mechanism in a PaSR simulation with IEM as micromixing model.

The PaSR simulation was performed with 500 particles, with mixing time of 8 ms. To start the simulation, the reactor particles are assumed to be unmixed, and the inlet particles are premixed before entering the reactor. Figs. 1 and 2 illustrate the performance of the reduced mechanism using IEM and CD models, respectively. It is observed that the reduced mechanism performs well when applied to mixing simulations and there is no significant deviation in the nature of the profiles. However, when compared to its performance under PSR conditions, it is observed that the accuracy has decreased considerably due to the broader range of conditions it is subjected to. Simulations were also performed with different mixing times, all of which revealed similar trends, which is consistent with the findings of Cannon et al. (1998) and Chen (1997).

Correa (1995) presents an extensive comparison of the performance of IEM and CD model in PaSR simulations. He observed that performance of these models become increasingly similar at higher mixing frequency. The most prominent difference observed between these two models

was that IEM model sustains combustion at lower frequency, while CD model blows out. Also, the mean quantities computed using IEM model are less noisy, as a consequence of the deterministic nature of the IEM model. Hence IEM model is chosen to describe micromixing in further simulations in this work.

5. Adaptive reduction

The analysis in the previous section showed that the reduced mechanism obtained under the assumption of perfect mixing can be applied for the cases of imperfect mixing conditions without much loss of accuracy. However, it is observed that in order to obtain a single reduced mechanism which retains considerable accuracy over the whole path, a large number of reactions still needs to be retained. Since importance of different reactions changes over the reaction time, to represent the entire trajectory by a single reaction set requires the inclusion of all the important reactions in

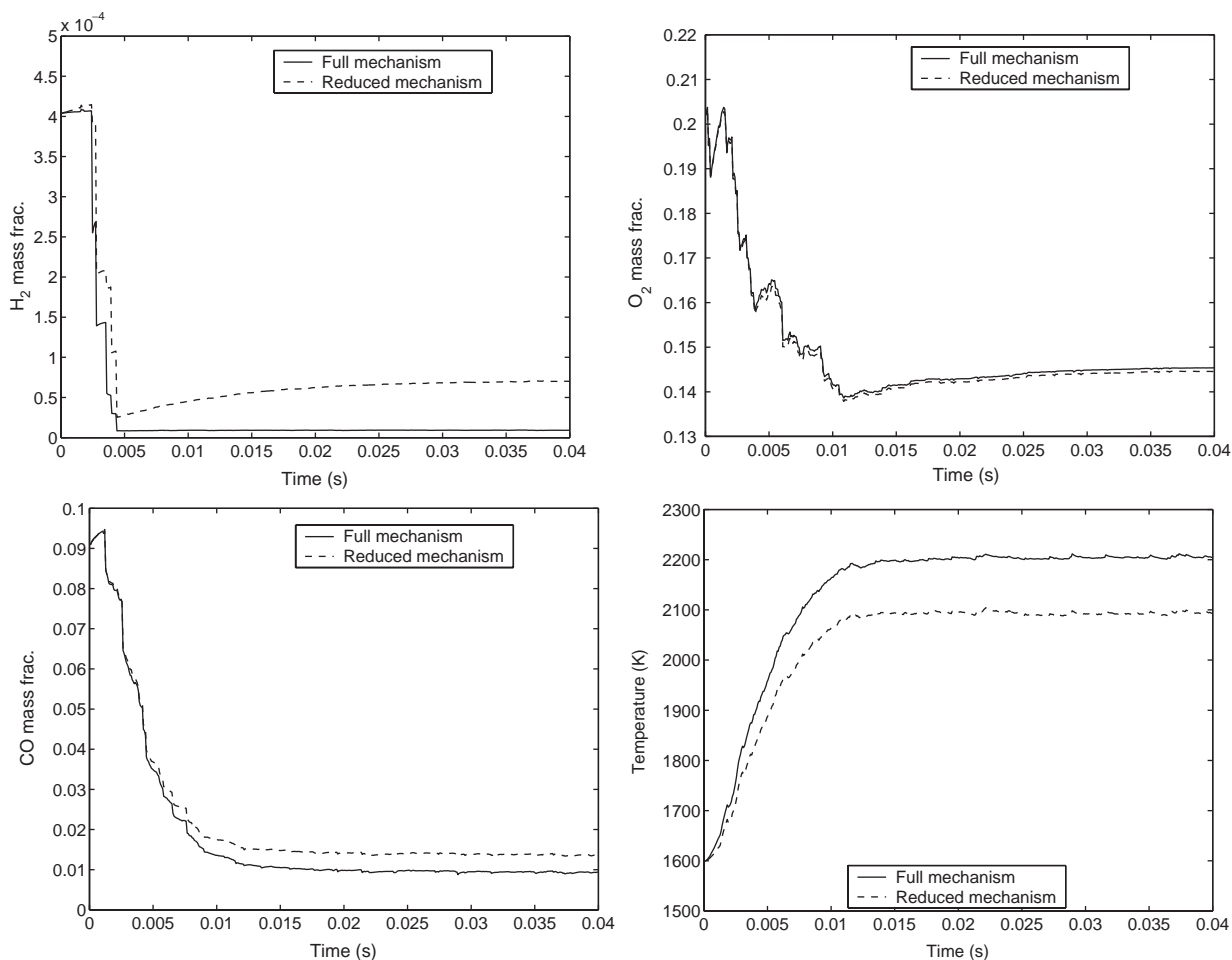


Fig. 2. Comparison between profiles of detailed and reduced mechanism in a PaSR simulation with CD as micromixing model.

the reduced set. However, if one can identify different reduced sets which are valid over different portions of the reaction trajectory, then it is possible to have better representation of the trajectory with smaller reaction sets. Thus instead of obtaining single reduced set valid over entire trajectory, the aim here is to obtain different reduced reaction sets which are valid over a limited time. The overall proposed approach of adaptive reduction consists of two steps as illustrated graphically in Fig. 3. In the first step the entire integration time is uniformly divided into certain number of intervals and a reduced reaction set is obtained for each of the interval. In the second step, these intervals are systematically refined to restrict the number of reactions in each of the reduced sets within a prescribed quantity. The optimization problem solved in the first step of the approach for each time interval is formulated as

$$\min_{\lambda \in A^{N_R}} \sum_{r=1}^{N_R} \lambda_r$$

$$\text{subject to } \chi \leq \frac{\delta}{N_{\text{int}}},$$

$$\text{where, } \chi = \left(\sum_{k \in \kappa} \int_{t_i^{N_{\text{int}}}}^{t_f^{N_{\text{int}}}} \left(\frac{y_k^{\text{reduced}}(t) - y_k^{\text{full}}(t)}{y_k^{\text{full}}(t)} \right)^2 dt + \int_{t_i^{N_{\text{int}}}}^{t_f^{N_{\text{int}}}} \left(\frac{T_k^{\text{reduced}}(t) - T_k^{\text{full}}(t)}{T_k^{\text{full}}(t)} \right)^2 dt \right)^{1/2}, \quad (17)$$

where y_k, T_k are obtained by reactor equations (3)–(7). N_{int} is user defined number of intervals into which the integration time was divided. $t_i^{N_{\text{int}}}$ and $t_f^{N_{\text{int}}}$ are the initial and final times for an interval, respectively, defining the range over which the differential equations needs to be integrated. To perform the reduction at each interval, the initial conditions for integration is set to the corresponding PSR conditions at that instant. The allowable error was also uniformly divided over each interval. This problem is solved following the procedure described in Section 2, and the results obtained by setting $N_{\text{int}} = 20$ is shown in Fig. 4, where the numbers correspond to the reaction numbers as shown in the appendix. Fig. 5 illustrates the temperature and H_2 profiles obtained by the adaptively reduced reaction sets. It is observed that

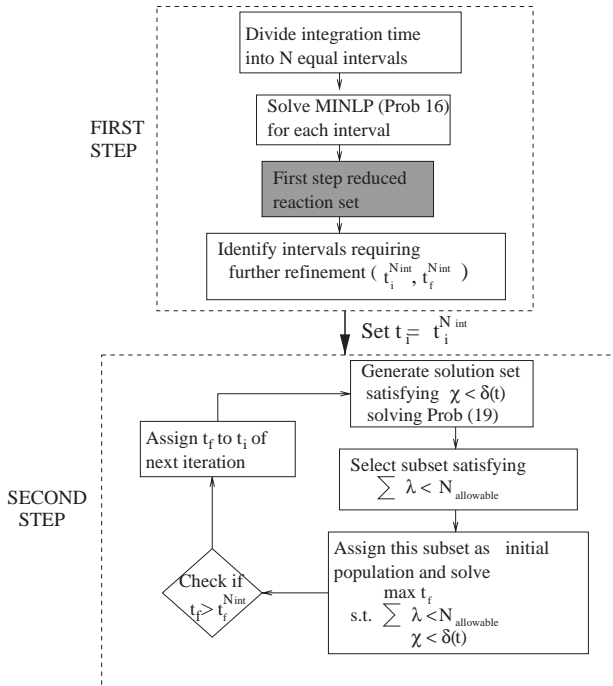
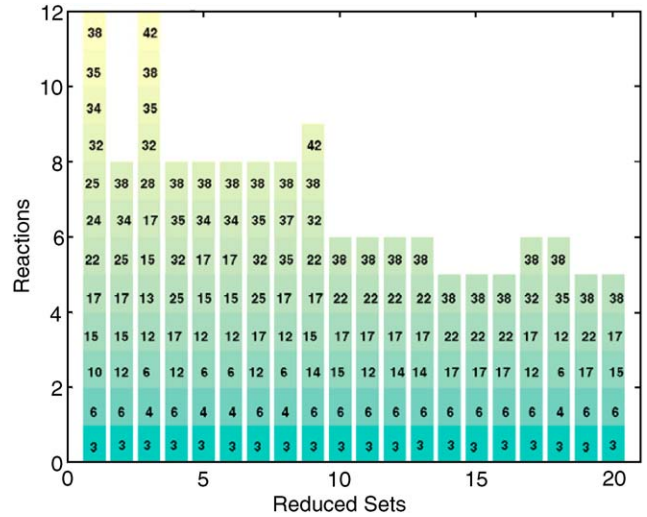


Fig. 3. Algorithm for adaptive reduction.

when the time domain is divided uniformly, a large number of reactions are retained in the reduced set for the initial stiff portion of the profile. However, after certain time the number of reactions retained in the reduced sets are consistently low. The intervals containing unacceptably high number of reactions are identified and passed on to the second step of the procedure for further refinement. The purpose of the second step is to identify the reduced set with acceptable number of reactions, and also determine the time over which the reduced set can be integrated to attain the prescribed

Fig. 4. Adaptively reduced reaction sets with $N_{int} = 20$ (numbers denote the reaction number retained in the reduced set).

accuracy. This is achieved by solving the following optimization problem:

$$\begin{aligned} & \max t_f \\ & \text{subject to } \sum_{r=1}^{N_R} \lambda_r < N_{allowable}, \\ & \chi \leq \delta^{int}(t) \end{aligned}$$

where, $\chi = \left(\sum_{k \in \kappa} \int_{t_i}^{t_f} \left(\frac{y_k^{reduced}(t) - y_k^{full}(t)}{y_k^{full}(t)} \right)^2 dt + \int_{t_i}^{t_f} \left(\frac{T_k^{reduced}(t) - T_k^{full}(t)}{T_k^{full}(t)} \right)^2 dt \right)^{1/2}$, (18)

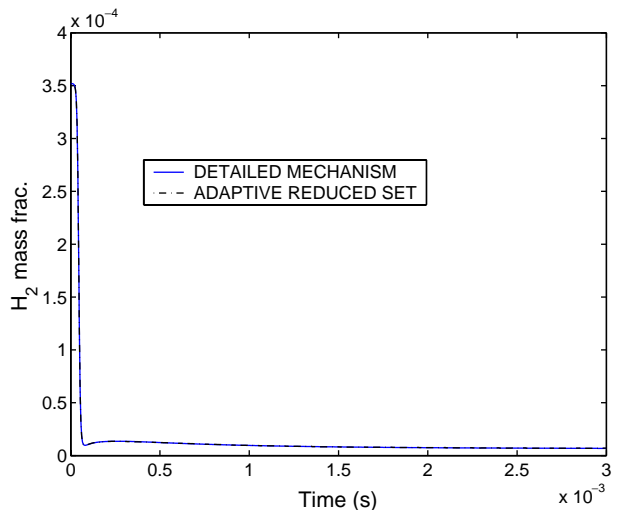
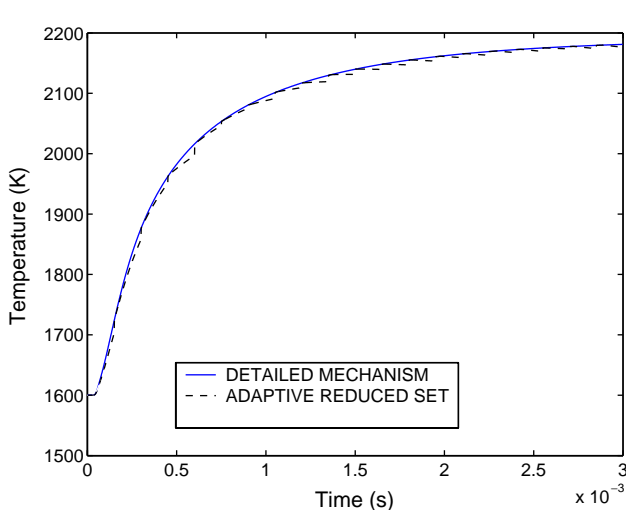


Fig. 5. Comparison between profiles of detailed mechanism with adaptively reduced mechanism in PSR simulation.

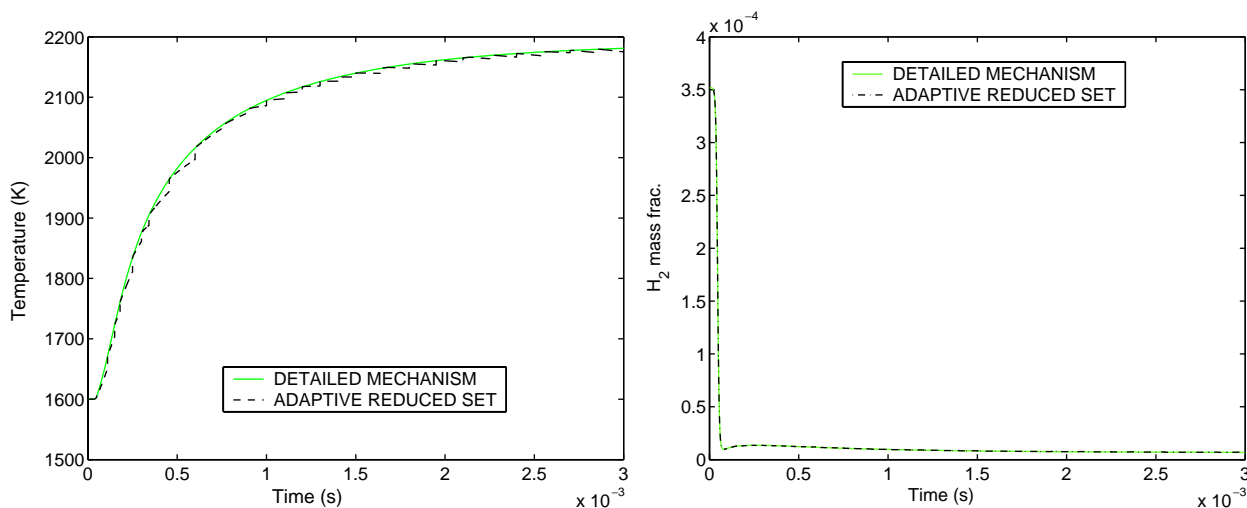


Fig. 7. Comparison between profiles of detailed mechanism with adaptively reduced mechanism in PSR simulation.

perfect mixing. These sets are stored along with the initial conditions and the integration time under which reduction is performed. Having constructed a library of reduced reaction sets, the mixing simulation can be performed, which proceeds by the following steps:

1. Fluid particles are selected at random and replaced by fresh feed at specified mass flow rate.
2. Fluid particles are allowed to mix according to IEM or CD mixing model at specified mixing frequency.
3. The mixed fluid particles are allowed to select an appropriate reduced reaction mechanism depending on the particle conditions.
4. The chosen mechanism is integrated over the incremental time step.

In the above algorithm, the throughflow and mixing steps are the same as for the case of single reaction mechanism. In the reaction step however, the additional problem of selecting the appropriate reduced mechanism has to be solved for each particle. There can be several possible criteria which governs the mechanism selection as appropriate under the particle conditions as analyzed in the next section.

6.1. Selection criteria for reduced mechanism

6.1.1. Single selection criterion

The simplest criterion is to select a mechanism based on the concentration of a particular species or temperature in the particle. Hence if particle temperature is chosen to be the selection criterion, then all the reduced mechanisms are characterized by the range of temperature over which it is integrated. While performing the mixing simulation, a mechanism which is valid for the particle temperature is selected. Stochastic simulation was performed for a mixture of CO/H₂ and air at a temperature of 1600 K; residence time = 8 ms;

mixing time = 8 ms. The PDF was represented by 500 particles and incremental time of 1.6×10^{-2} ms. The profiles are compared by evaluating an error value, which is the integrated difference between the full profile and the reduced profile of all the observed species. Fig. 8 illustrates the performance of the adaptively reduced set with temperature as the selection criterion, and compares it with a single reduced set used over the entire integration time. It can be seen that the adaptive chemistry performs much better, resulting in an order of magnitude reduction of error from 1.73944 using a single reduced set to 0.177437 using an adaptive scheme. However, the problem associated with this approach is that the composition space accessed by the PaSR is much larger than that accessed by the PSR. Hence the reduced sets generated by the above procedure covers a very small region of the entire accessed space. In the present simulation, for the temperatures not covered by the reduced sets, the chosen reduced set was the one which was closest to the particle condition.

Similar simulations were performed with the different watched species as the selection criteria, and the results are presented in Fig. 9. Fig. 10 presents a comparison of single step reduction with adaptively reduced sets, and it also illustrates the importance of appropriate selection criteria. It is observed that even though the adaptively reduced sets has the same average number of reactions as the single reduced set, the performance of adaptive reduction is better than that of the later. It is also observed that when temperature and H₂ concentration are chosen to be the selection criteria, the species profiles were predicted with higher accuracy as compared to the selection criteria based on O₂ and CO concentration. To evaluate the prediction of individual species, Figs. 11–13 are presented, that compare the performance of different selection criteria on the prediction of individual species concentration. It is observed that profiles based on temperature and H₂ concentration were more

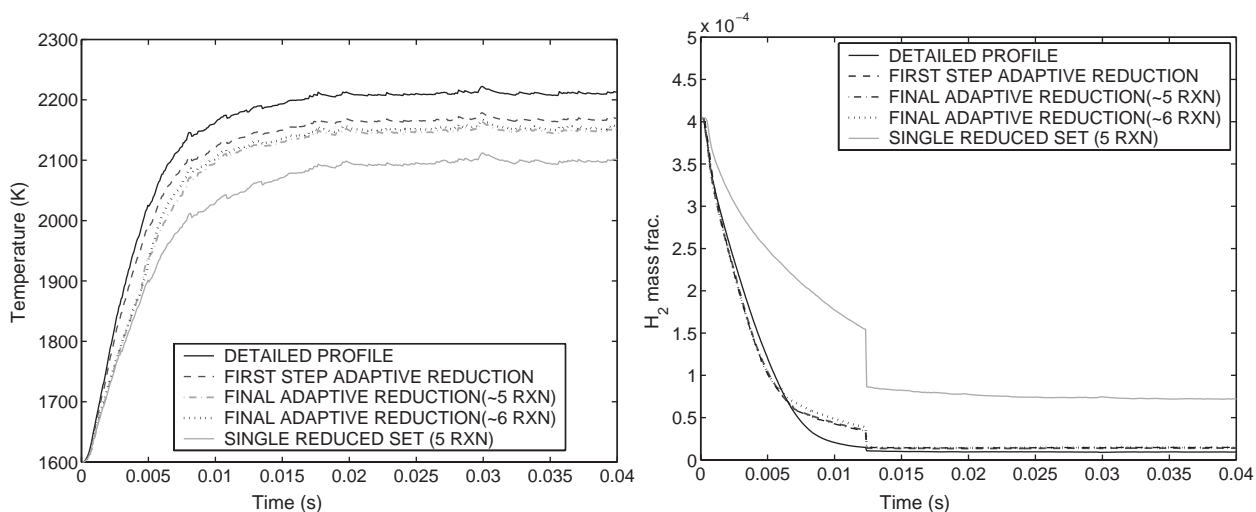


Fig. 8. Comparison between profiles of different reduced sets in PaSR simulation, with temperature as selection criterion.

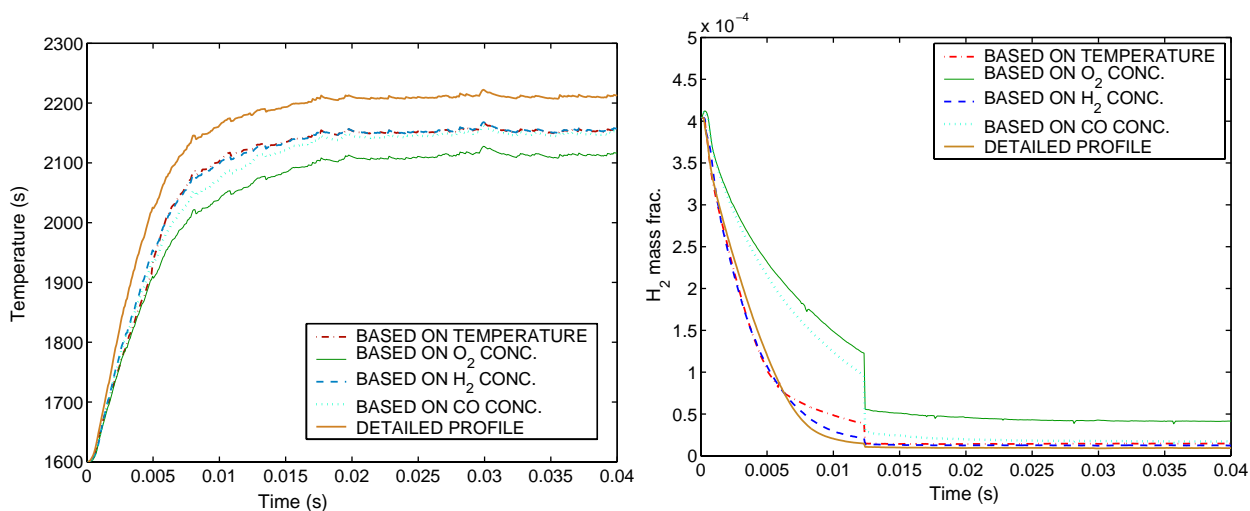


Fig. 9. Comparison between profiles of different reduced sets in PaSR simulation, with different species concentration as selection criterion.

accurate than that based on CO and O₂ concentration. It is also observed that the profiles of temperature, H₂ and CO₂ are predicted better with H₂ as selection criterion. Regarding CO profile both temperature and H₂ concentration as selection basis had similar performance, whereas O₂ profile was better predicted by temperature as the selection criterion.

Similar simulations were performed for different mixing time of 1.6 ms, and the results are presented in Fig. 14. For this case it is observed that all the selection criteria based on different species concentration were having comparable performance, and were better than the performance of single reduced reaction set. Though the overall performance was best for H₂ concentration as selection basis, when individual species profiles are examined it is observed that mechanism selection based on particle temperature results in better prediction of temperature, CO and CO₂ profile, whereas H₂ and O₂ profiles are more accurately

predicted by selection based on H₂ concentration. From the presented results it can be summarized that the selection which is based on a single species concentration or temperature does not provide the best profile of all the observed species.

6.1.2. Combined error value as selection criteria

A more involved criterion would be to estimate the error encountered by a particular mechanism when it is applied under the particle conditions, and select a mechanism having minimum error. The reduced mechanisms are obtained under certain initial conditions, at which when integrated over a certain time it satisfies the prescribed error constraint. Hence, when these mechanisms are integrated from different initial conditions an additional error is encountered, referred to as the deviation error, and

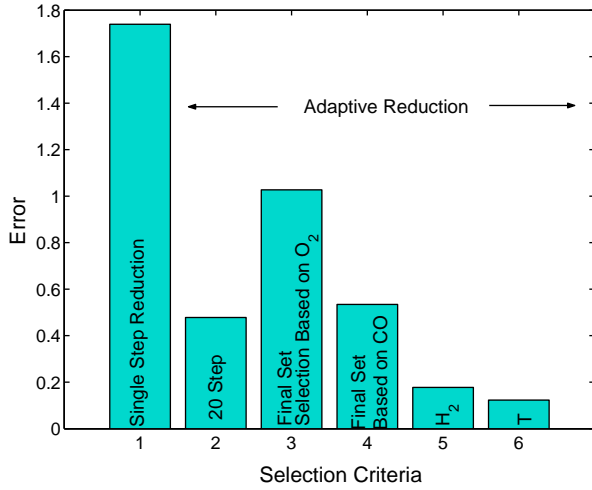


Fig. 10. Comparison of the error incurred by using single step reduction and adaptive reduction with different selection criteria in a PaSR simulation, $t_{\text{mix}} = 0.008$ s.

expressed as

$$Q(\alpha) = \sum_{j=1}^q \sum_{i=1}^m \left[\frac{\xi_{i,j}(\alpha) - \xi_{i,j}(\alpha^0)}{\xi_{i,j}(\alpha^0)} \right]^2, \quad (21)$$

where $\xi_{i,j}(\alpha) = \xi_i(t_j, \alpha)$ denotes the error between detailed and reduced mechanism at each selected time point (t_j , $j = 1, 2, \dots, q$) and for each of the m observed species. α is a measure of initial species concentration y_i , given as

$$\alpha_i = \ln y_i, \quad i = 1, 2, \dots, p. \quad (22)$$

For the present simulation, initial concentrations of H₂, O₂ and CO along with initial temperature were considered for

evaluation of $Q(\alpha)$. $\xi_{i,j}(\alpha)$ can be seen as the deviation of the reduced profile from the detailed profile under particle conditions, and $\xi_{i,j}(\alpha^0)$ as the same deviation under the nominal condition at which reduction was performed. The classical Gauss approximation gives (Vajda, Valko, & Turanyi, 1985)

$$Q(\alpha) \approx \tilde{Q}(\alpha) = (\Delta\alpha)^T S^T S (\Delta\alpha), \quad (23)$$

where $\Delta\alpha_i = \alpha_i - \alpha_i^0$, which is the deviation of the particle condition from the nominal condition of reduction. S is the array of normalized sensitivities at each time points t_1, t_2, \dots, t_q ,

$$S = \begin{bmatrix} S_1 \\ S_2 \\ \vdots \\ S_q \end{bmatrix},$$

$$S_i = \begin{bmatrix} \frac{\partial \ln \xi_{1,i}}{\partial \ln \alpha_1} & \frac{\partial \ln \xi_{1,i}}{\partial \ln \alpha_2} & \cdots & \frac{\partial \ln \xi_{1,i}}{\partial \ln \alpha_p} \\ \frac{\partial \ln \xi_{2,i}}{\partial \ln \alpha_1} & \frac{\partial \ln \xi_{2,i}}{\partial \ln \alpha_2} & \cdots & \frac{\partial \ln \xi_{2,i}}{\partial \ln \alpha_p} \\ \vdots & \vdots & \ddots & \vdots \\ \frac{\partial \ln \xi_{m,i}}{\partial \ln \alpha_1} & \frac{\partial \ln \xi_{m,i}}{\partial \ln \alpha_2} & \cdots & \frac{\partial \ln \xi_{m,i}}{\partial \ln \alpha_p} \end{bmatrix}.$$

By performing singular value decomposition of $S^T S$ it can be expressed as

$$S^T S = U^T A U, \quad (24)$$

where A is a diagonal matrix formed by the eigenvalues λ_i of $S^T S$ and U denotes the matrix of orthonormal eigenvectors

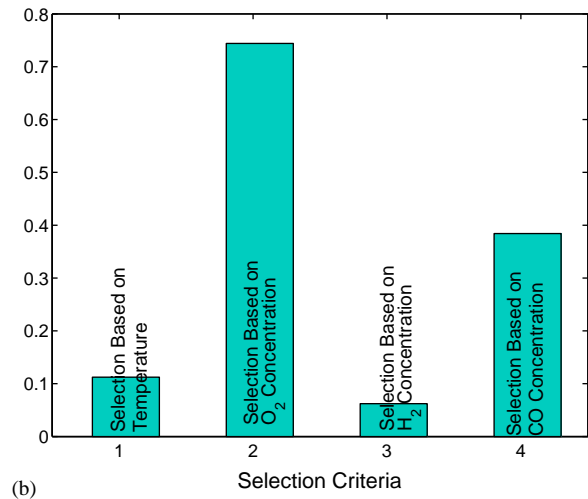
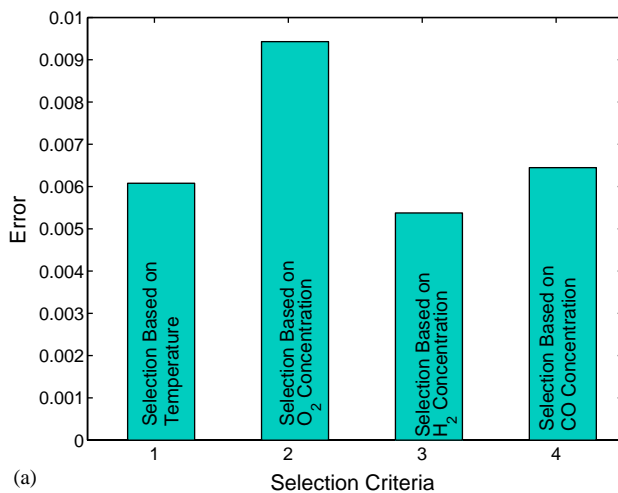


Fig. 11. Comparison of the error incurred in the prediction of (a) temperature and (b) H₂ profile by using different selection criteria.

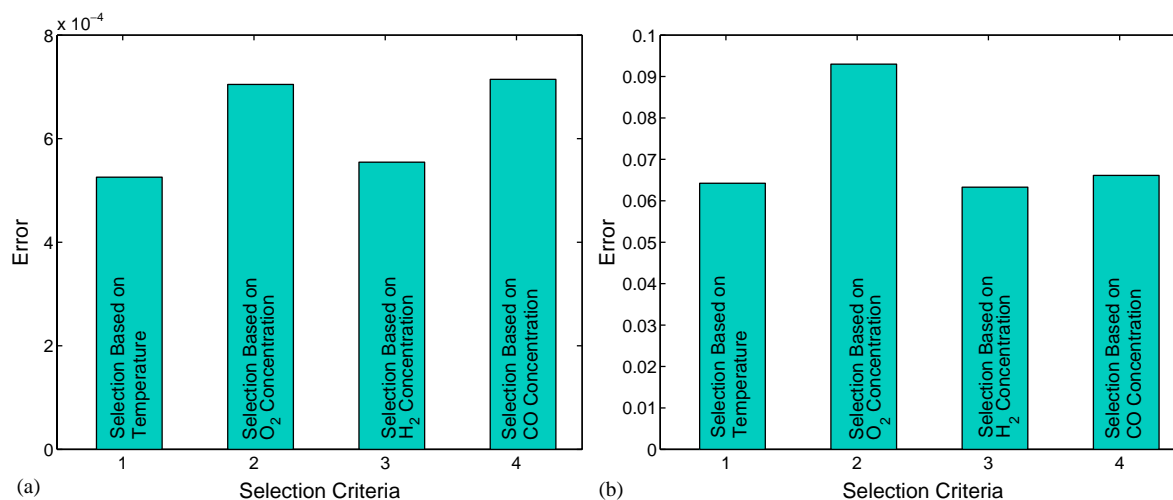


Fig. 12. Comparison of the error incurred in the prediction of (a) O₂ and (b) CO profile by using different selection criteria.

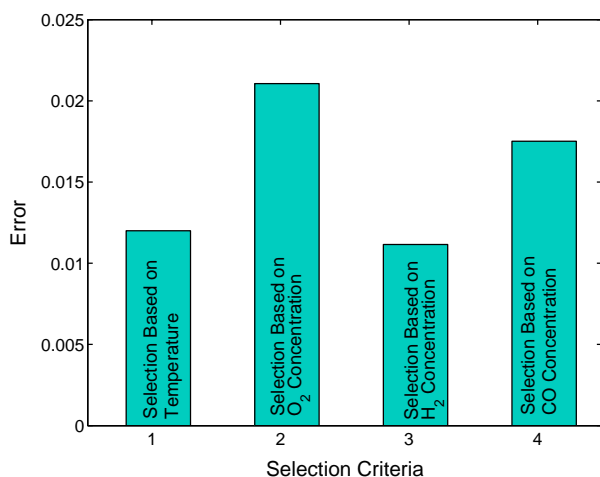


Fig. 13. Comparison of the error incurred in the prediction of CO₂ profile by using different selection criteria.

u_i , $i = 1, 2, \dots, p$. Bard (1974) defined the principal components as

$$\Psi = U^T \alpha \quad (25)$$

using which $\tilde{Q}(\Psi)$ can be expressed as

$$\tilde{Q}(\Psi) = \sum_{i=1}^p \lambda_i \|\Delta \Psi_i\|^2. \quad (26)$$

Hence knowing the eigenvalues and eigenvectors of the sensitivity matrix, enables one to approximately estimate the deviation error $Q(\alpha)$. After executing the reduction step, the above analysis is performed for each of the reduced mechanisms, and the eigenvalue and eigenvector information is stored. While performing the mixing simulation, each particle at each incremental time step visits all the reduced mechanisms and calculates the expected deviation error ($Q(\alpha)$) based on the particle conditions, and selects the mechanism

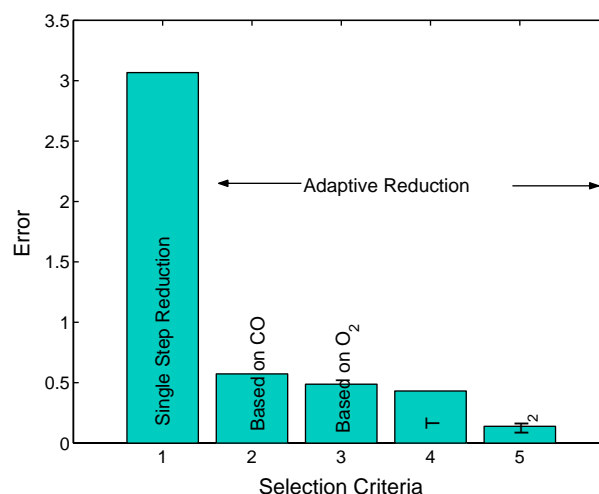


Fig. 14. Comparison of the error incurred by using single step reduction and adaptive reduction with different selection criteria in a PaSR simulation, $t_{\text{mix}} = 0.0016$ s.

having the minimum value of error. Fig. 15 illustrates the performance of this selection criterion and compares it with profiles obtained by using single reduced reaction set, which is found to have a larger error (1.74) as compared to the former, which has an error of 0.0998. Fig. 16 illustrates the performance of the combined error selection criterion in the prediction of the *unwatched* species and it is observed that although the reduced set was not optimized for these species, still the reduced profiles match well with the detailed profiles.

Fig. 17 compares the performance of combined error with that of single species selection criterion on the basis of overall error. It is observed that for both mixing times considered, the selection based on combined error analysis performed better than the best of single species selection

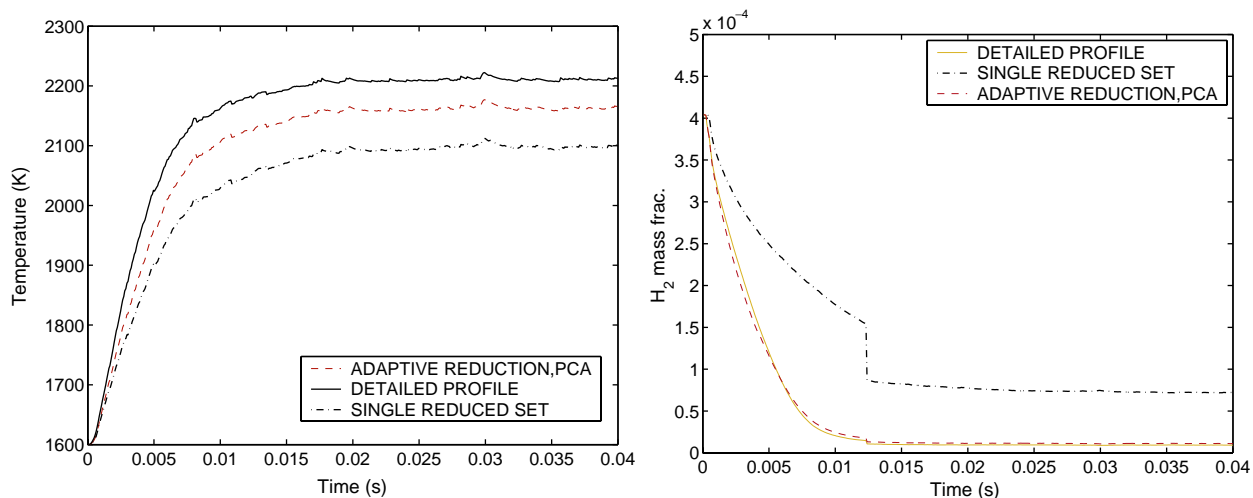


Fig. 15. Comparison between profiles obtained by using a single reduced set and adaptively reduced set using combined error as selection criterion.

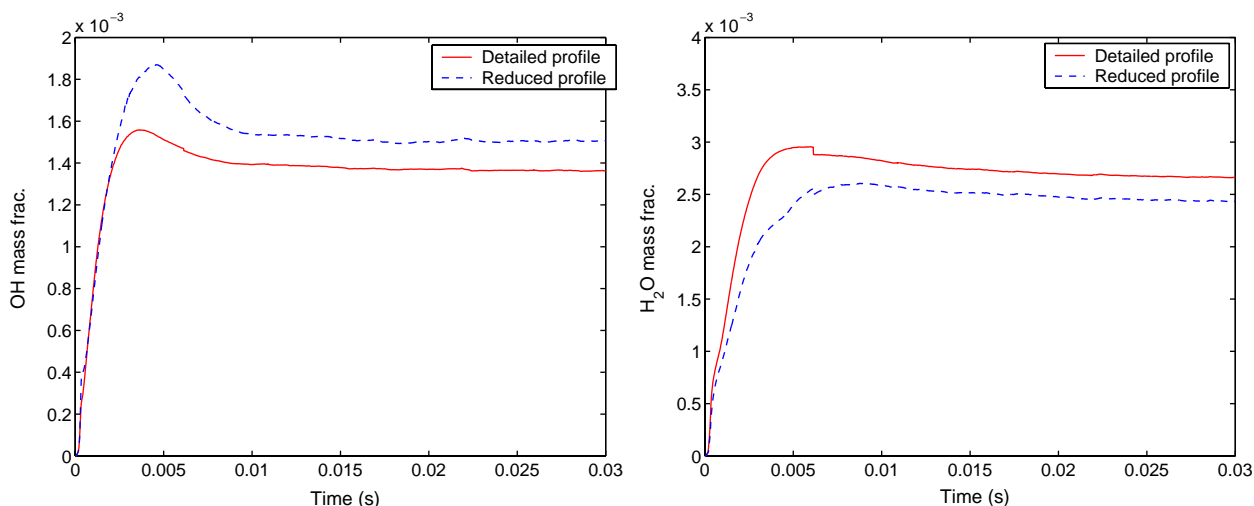


Fig. 16. Performance of adaptive reduction in the prediction of nonwatched species.

criteria. To understand the performance in predicting individual species profile, Fig. 18 illustrates the percentage error reduction obtained by using combined error analysis over the best prediction possible by using single species concentration as mechanism selection criterion. For all the cases considered it is observed that the performance of combined error as selection criterion is superior to selecting a mechanism based on single species concentration or temperature. The presented results were obtained by considering 35 reduced reaction sets, and while performing the flow simulation, all the reduced models have to be evaluated to select the best one. This selection step increases the CPU requirement at each time step by 0.06 ms for a set of 35 reactions, and is expected to increase linearly with the number of reduced reaction models. This is considerably less as compared to the CPU savings resulting from the use of reduced reaction models.

7. Discussion

The focus of the presented work was to develop multiple reduced reaction sets to cover different regions of the reaction trajectory, in order to have higher accuracy in the prediction of system performance. Such an adaptive reduction problem was formulated as an integer optimization problem, solution procedure of which is discussed in detail. Such an adaptive reduced set of reactions can be easily implemented in reactive flow simulation. The present study is restricted to PaSR simulation with IEM model to describe micromixing effects. The behavior of the reduced sets in the mixing model was analyzed and different criteria for the selection of appropriate mechanism are evaluated. It was always observed that adaptively reduced reactions perform better than a single reduced set, even if the average number of reactions in the adaptive set is the same as that of the single set.

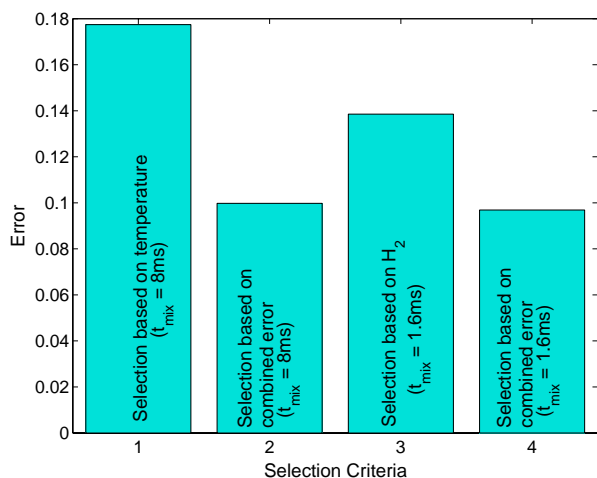


Fig. 17. Comparison of the error incurred by using adaptive reduction with combined error selection criterion and single species selection criterion, at different mixing times.

Also, the performance of the adaptive reduction can be significantly improved by defining an appropriate criterion for mechanism selection. In the present work it was observed that selection based on combined error measure performs better than that based on single species concentration. There are still a number of issues that needs to be addressed to further improve the performance of adaptive reduction.

The basic steps of the proposed approach consist of obtaining reduced reaction sets under the assumption of perfect mixing conditions and then performing the mixing simulation by judicious selection of appropriate reduced reaction sets. Hence the reduced sets are determined for the range of conditions accessed by the PSR. However, it is observed that the particles in the PaSR simulation accesses a much larger region in the composition space, as compared to a PSR. Moreover, when PaSR is used with IEM model,

the particle composition becomes a unique function of its age, resulting in a one-dimensional manifold. The pairwise mixed stirred reactor (PMSR) (Pope, 1997) was developed to overcome this difficulty and yield a larger accessed region, providing a more stringent test for combustion chemistry, which is currently under investigation in our studies. Fig. 19 presents a comparison of the temperature-CO and temperature-H₂ space accessed by each particle at each time interval considered in the simulation of the PSR and PaSR. This can be a serious restriction since the reduced sets are being used at conditions very different from the conditions at which they are reduced, and hence it might not be valid. For example, while performing the mixing simulation with single species composition as selection criterion, conditions were encountered out of range of PSR conditions. For those cases the chosen mechanism was the one valid under conditions closest to the particle condition. When considering the combined error as defined by Eq. (21) as the selection criterion, the chosen mechanism is always the one with minimum error, which itself might be large enough to incorporate considerable inaccuracy in prediction. Hence it is important to determine the feasible region of the reduced set, which requires the determination of the range of conditions over which a particular reduced set can be applied while retaining the desired accuracy. Knowledge of the feasible region of each reduced set is likely to increase the accuracy of the presented procedure, since one can choose a mechanism feasible under the particle conditions. This will require (1) accurate representation of the feasible region of each reduced set and (2) generation of sufficient reduced sets to cover the entire accessed region of the PaSR. Sirdeshpande et al. (2001) presented a detailed analysis of feasibility problem of mechanism reduction and quantification of feasible region. This approach can be applied to address the feasible region of reduced sets, but it becomes computationally demanding with increasing dimensions of the composition

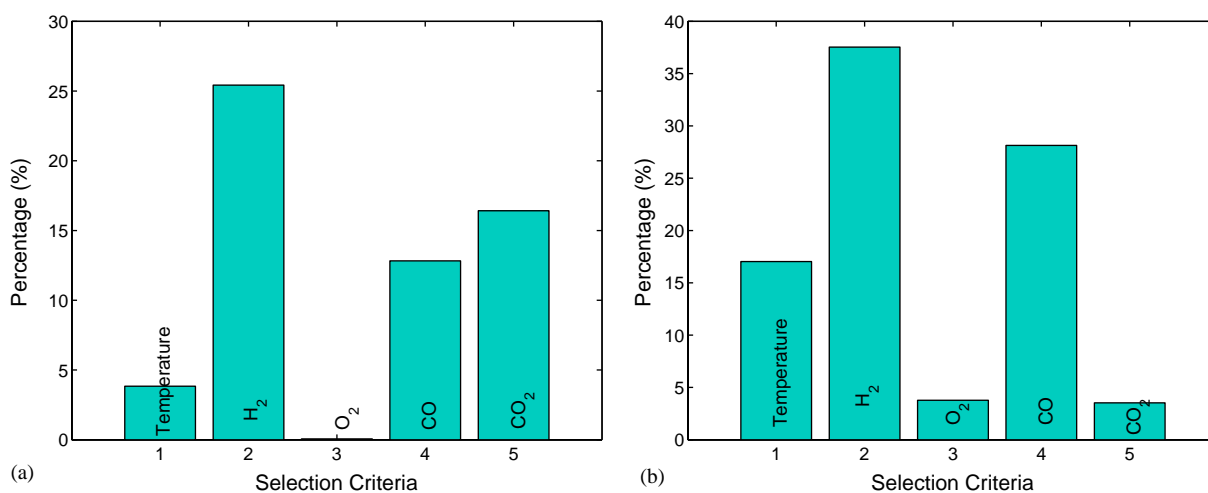


Fig. 18. Comparison of error reduction obtained by using combined error selection criterion and the best prediction possible by using single species selection criterion, (a) $t_{mix} = 0.008$ s and (b) $t_{mix} = 0.0016$ s.

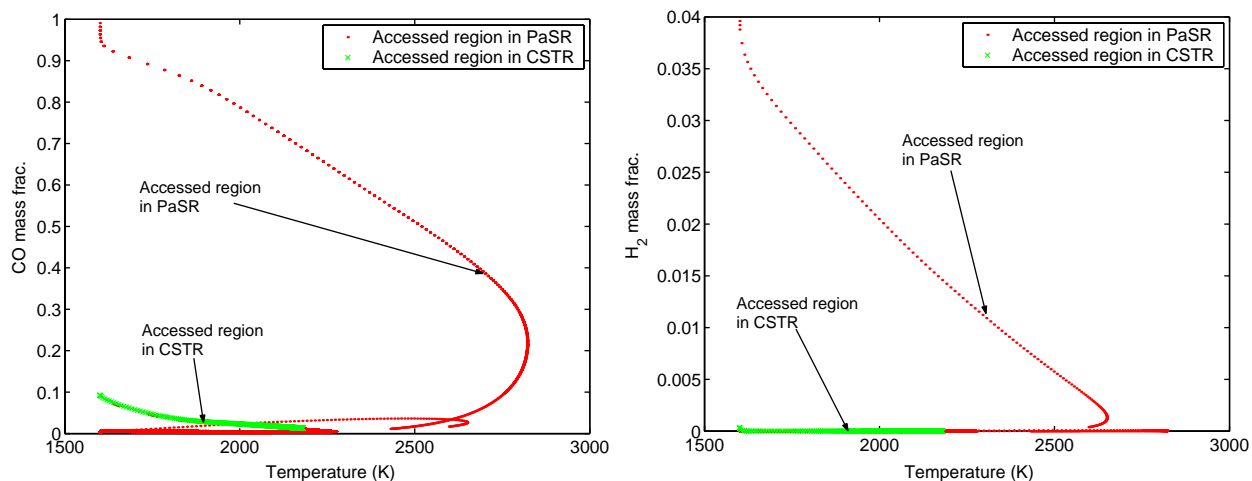


Fig. 19. Comparison of composition space accessed by PSR and PaSR.

space. Current research is directed towards reducing the dimension of feasibility analysis and better quantification of feasible region using the ideas of PCA. It is expected that if a chosen mechanism is always valid at the conditions under which it is applied, then the Δt required for convergence of the profiles will be same as that for detailed mechanism.

As discussed in Section 6, the reduced set chosen by an appropriate criterion is integrated over the incremental time step Δt . However, if the integration time t_f , as obtained from Problem (18), for a particular reduced set is less than Δt , then integrating the mechanism over the entire Δt is likely to introduce additional error. To avoid that, the approach adopted in present work is to integrate the chosen reduced set until the corresponding t_f , and perform the selection step again at the end of t_f . Hence, step (4) of the mixing simulation will now consists of multiple selection and integration steps. However, since the final goal is to incorporate the proposed strategy in a CFD code, the importance of this issue will be decided by the incremental time stepping required in the CFD code. If the CFD code requires time steps larger than t_f , then one has to choose between sacrificing accuracy by integrating until Δt or integrating a larger reaction set.

The mechanism reduction problem addressed in this work is primarily to minimize the total number of reactions in a particular network. An alternative representation for minimizing the number of species present in the network is also presented with regard to methane mechanism. Reducing the number of species is of primary importance since it directly reduces the number of ordinary differential equations required to model the reactive flow problem. In the formulation of reaction reduction, species reduction occurs as a consequence of reaction elimination, since a species will be removed from the network if it participates only in the eliminated reactions. Following the present formulation of minimization of number of reactions, it is possible to analyze the family of solutions for total number of species, and select

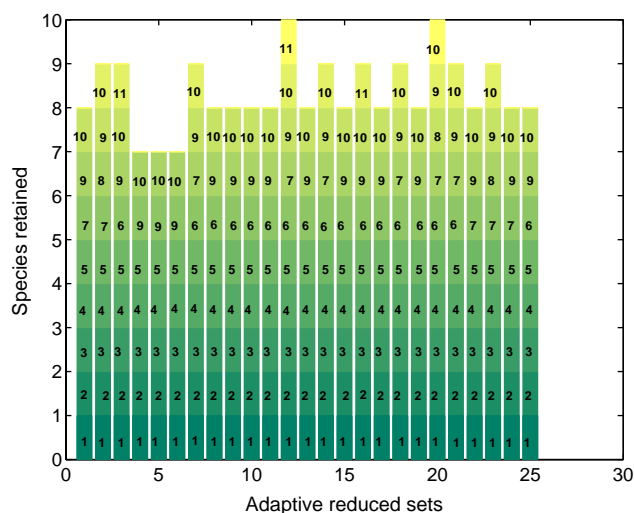


Fig. 20. Species retained in adaptive reduced set.

the one with minimum number of species. However, a better approach will be to perform the adaptive reduction for the problem of species reduction wherein the objective would be to minimize the total number of species. Fig. 20 presents the species retained by the adaptive reduced sets with allowable number of reactions equal to 6. It can be observed from Fig. 20 that different reduced sets retain different species, as a consequence of which different time steps will have different involved species. For example, if the first reduced set is selected at a certain time step, followed by the selection of second reduced set in the next time step, then the second time step will involve an additional specie (8), which was absent in the earlier time step. This problem is addressed by allowing all the species to participate in the mixing step, and the only implication of the absence of a species from a reduced set is that it does not participate in the reaction step. Hence the concentration of a nonparticipating species

is unaltered by the reaction step. Hence it is observed in Fig. 16 that there is no discontinuity in the mean profile of H₂O (specie 6), even though it is not present in all the reaction sets.

Acknowledgements

The authors gratefully acknowledge financial support from the donors of the Petroleum Research Fund

administered by the ACS and Office of Naval Research under the contract N00014-03-1-0207. The Genetic Algorithm code used in this paper was originally developed by David L. Carroll.

Appendix.

The CO/H₂/air mechanism details are shown in Tables 1 and 2.

Table 1
Species involved in CO/H₂/air mechanism

Species no.	1	2	3	4	5	6	7	8	9	10	11	12	13	14
Species	H ₂	H	O	O ₂	OH	H ₂ O	HO ₂	H ₂ O ₂	CO	CO ₂	HCO	CH ₂ O	N ₂	Ar

Table 2
The full CO/H₂/air mechanism

	Reactions considered	$k_{f,i} = A_i e^{-E_i/RT} T^{b_i}$		
		A_i	b_i	E_i/R
1.	2O + M ↔ O ₂ + M H ₂ enhanced by 2.400 H ₂ O enhanced by 1.540 × 10 ¹ CO enhanced by 1.75 CO ₂ enhanced by 3.600 AR enhanced by 8.300 × 10 ⁻¹	1.20 × 10 ¹⁷	-1.0	0.0
2.	O + H + M ↔ OH + M H ₂ enhanced by 2.000 H ₂ O enhanced by 6.000 CO enhanced by 1.500 CO ₂ enhanced by 2.00 AR enhanced by 7.000 × 10 ⁻¹	5.00 × 10 ¹⁷	-1.0	0.0
3.	O + H ₂ ↔ H + OH	5.00 × 10 ⁴	2.67	6290.0
4.	O + HO ₂ ↔ OH + O ₂	2.00 × 10 ¹³	0.0	0.0
5.	O + H ₂ O ₂ ↔ OH + HO ₂	9.63 × 10 ⁶	2.0	4000.0
6.	O + CO + M ↔ CO ₂ + M H ₂ enhanced by 2.000 O ₂ enhanced by 6.000 H ₂ O enhanced by 6.000 CO enhanced by 1.500 CO ₂ enhanced by 3.500 AR enhanced by 5.000 × 10 ⁻¹	6.02 × 10 ¹⁴	0.0	3000.0
7.	O + HCO ↔ OH + CO	3.00 × 10 ¹³	0.0	0.0
8.	O + HCO ↔ H + CO ₂	3.00 × 10 ¹³	0.0	0.0
9.	O + CH ₂ O ↔ OH + HCO	3.90 × 10 ¹³	0.0	3540.0
10.	O ₂ + CO ↔ O + CO ₂	2.50 × 10 ¹²	0.0	47800.0
11.	O ₂ + CH ₂ O ↔ HO ₂ + HCO	1.00 × 10 ¹⁴	0.0	40000.0
12.	H + O ₂ + M ↔ HO ₂ + M O ₂ enhanced by 0.000 H ₂ O enhanced by 0.000 CO enhanced by 7.500 × 10 ⁻¹ CO ₂ enhanced by 1.500 N ₂ enhanced by 0.000 AR enhanced by 0.000	2.80 × 10 ¹⁸	-0.860	0.0
13.	H + 2O ₂ ↔ HO ₂ + O ₂	3.00 × 10 ²⁰	-1.72	0.0
14.	H + O ₂ + H ₂ O ↔ HO ₂ + H ₂ O	9.38 × 10 ¹⁸	-0.76	0.0
15.	H + O ₂ + N ₂ ↔ HO ₂ + N ₂	3.75 × 10 ²⁰	-1.72	0.0
16.	H + O ₂ + AR ↔ HO ₂ + AR	7.00 × 10 ¹⁷	-0.8	0.0
17.	H + O ₂ ↔ O + OH	8.30 × 10 ¹³	0.0	14413.0

Table 2 (continued)

	Reactions considered	$k_{f,i} = A_i e^{-E_i/RT} T^{b_i}$		
		A_i	b_i	E_i/R
18.	2H + M \leftrightarrow H ₂ + M H ₂ enhanced by 0.000 H ₂ O enhanced by 0.000 CO ₂ enhanced by 0.000 AR enhanced by 6.300×10^{-1}	1.00×10^{18}	-1.0	0.0
19.	2H + H ₂ \leftrightarrow 2H ₂	9.00×10^{16}	-0.6	0.0
20.	2H + H ₂ O \leftrightarrow H ₂ + H ₂ O	6.00×10^{19}	-1.25	0.0
21.	2H + CO ₂ \leftrightarrow H ₂ + CO ₂	5.50×10^{20}	-2.0	0.0
22.	H + OH + M \leftrightarrow H ₂ O + M H ₂ enhanced by 7.300×10^{-1} H ₂ O enhanced by 3.650 AR enhanced by 3.800×10^{-1}	2.20×10^{22}	-2.0	0.0
23.	H + HO ₂ \leftrightarrow O + H ₂ O	3.97×10^{12}	0.0	671.0
24.	H + HO ₂ \leftrightarrow O ₂ + H ₂	2.80×10^{13}	0.0	1068.0
25.	H + HO ₂ \leftrightarrow 2OH	1.34×10^{14}	0.0	635.0
26.	H + H ₂ O ₂ \leftrightarrow HO ₂ + H ₂	1.21×10^7	2.0	5200.0
27.	H + H ₂ O ₂ \leftrightarrow OH + H ₂ O	1.00×10^{13}	0.0	3600.0
28.	H + HCO(+M) \leftrightarrow CH ₂ O(+M) <i>Low pressure limit:</i> 0.13500×10^{25} -0.25700×10^{01} 0.14250×10^4 <i>TROE centering:</i> 0.78240 0.27100×10^3 0.27550×10^4 0.65700×10^4 H ₂ enhanced by 2.000 H ₂ O enhanced by 6.000 CO enhanced by 1.500 CO ₂ enhanced by 2.000 AR enhanced by 7.000×10^{-1}	1.09×10^{12}	0.48	-260.0
29.	H + HCO \leftrightarrow H ₂ + CO	7.34×10^{13}	0.0	0.0
30.	H + CH ₂ O \leftrightarrow HCO + H ₂	2.30×10^{10}	1.05	3275.0
31.	H ₂ + CO(+M) \leftrightarrow CH ₂ O(+M) <i>Low pressure limit:</i> 0.50700×10^{28} -0.34200×10^1 0.84350×10^5 <i>TROE centering:</i> 0.93200 0.19700×10^3 0.15400×10^4 0.10300×10^5 H ₂ enhanced by 2.000 H ₂ O enhanced by 6.000 CO enhanced by 1.500 CO ₂ enhanced by 2.000 AR enhanced by 7.000×10^{-1}	4.30×10^7	1.5	79600.0
32.	OH + H ₂ \leftrightarrow H + H ₂ O	2.16×10^8	1.5	3430.0
33.	2OH(+M) \leftrightarrow H ₂ O ₂ (+M) <i>Low pressure limit:</i> 0.23000×10^{19} -0.90000 -0.17000×10^4 <i>TROE centering:</i> 0.73460 0.94000×10^2 0.17560×10^4 0.51820×10^4 H ₂ enhanced by 2.000 H ₂ O enhanced by 6.000 CO enhanced by 1.500 CO ₂ enhanced by 2.000 AR enhanced by 7.000×10^{-1}	7.40×10^{13}	-0.37	0.0
34.	2OH \leftrightarrow O + H ₂ O	3.57×10^4	2.4	-2110.0
35.	OH + HO ₂ \leftrightarrow O ₂ + H ₂ O	2.90×10^{13}	0.0	-500.0
36.	OH + H ₂ O ₂ \leftrightarrow HO ₂ + H ₂ O	1.75×10^{12}	0.0	320.0
37.	OH + H ₂ O ₂ \leftrightarrow HO ₂ + H ₂ O	5.80×10^{14}	0.0	9560.0
38.	OH + CO \leftrightarrow H + CO ₂	4.76×10^7	1.228	70.0
39.	OH + HCO \leftrightarrow H ₂ O + CO	5.00×10^{13}	0.0	0.0
40.	OH + CH ₂ O \leftrightarrow HCO + H ₂ O	3.43×10^9	1.18	-447.0
41.	2HO ₂ \leftrightarrow O ₂ + H ₂ O ₂	1.30×10^{11}	0.0	-1630.0
42.	2HO ₂ \leftrightarrow O ₂ + H ₂ O ₂	4.20×10^{14}	0.0	12000.0
43.	HO ₂ + CO \leftrightarrow OH + CO ₂	1.50×10^{14}	0.0	23600.0
44.	HO ₂ + CH ₂ O \leftrightarrow HCO + H ₂ O ₂	1.00×10^{12}	0.0	8000.0
45.	HCO + H ₂ O \leftrightarrow H + CO + H ₂ O	2.244×10^{18}	-1.0	17000.0

Table 2 (continued)

	Reactions considered	$k_{f,i} = A_i e^{-E_i/RT} T^{b_i}$		
		A_i	b_i	E_i/R
46.	HCO + M \leftrightarrow H + CO + M H ₂ enhanced by 2.000 H ₂ O enhanced by 0.000 CO enhanced by 1.500 CO ₂ enhanced by 2.000	1.87×10^{17}	-1.0	17000.0
47.	HCO + O ₂ \leftrightarrow HO ₂ + CO	7.60×10^{12}	0.0	400.0

Units: E_i (K), A_i (mol cm s K).

Species X Enhanced by y refers to enhancement factor for third body reactions.

Please refer CHEMKIN documentation Kee et al. (1996) for details.

References

- Androulakis, I. P. (2000). Kinetic mechanism reduction based on an integer programming approach. *A.I.Ch.E. Journal*, 46, 361.
- Bard, Y. (1974). *Nonlinear parameter estimation*. New York: Academic Press.
- Borghgi, R. (1988). Turbulent combustion modelling. *Progress in Energy and Combustion Science*, 14, 245.
- Cannon, S. M., Brewster, B. S., & Smoot, L. D. (1998). Stochastic modeling of co and no premixed methane combustion. *Combustion and Flame*, 113, 135.
- Chen, J. Y. (1997). Stochastic modeling of partially stirred reactors. *Combustion Science and Technology*, 122, 63.
- Correa, S. M. (1993). Turbulence-chemistry interactions in the intermediate regime of premixed combustion. *Combustion and Flame*, 93, 41.
- Correa, S. M. (1995). A direct comparison of pair-exchange and iem models in premixed combustion. *Combustion and Flame*, 103, 194.
- Curl, R. L. (1963). Dispersion phase mixing i: Theory and effects in simple reactor. *A.I.Ch.E. Journal*, 9, 175.
- Dopazo, C. (1975). Probability density function approach for a turbulent axisymmetric heated jet centerline evolution. *Physics of Fluids*, 18, 397.
- Edwards, K., Edgar, T., & Manousiouthakis, V. I. (1998). Kinetic model reduction using genetic algorithm. *Computers and Chemical Engineering*, 22, 239.
- Edwards, K., Edgar, T. F., & Manousiouthakis, V. I. (2000). Reaction mechanism simplification using mixed-integer nonlinear programming. *Computers and Chemical Engineering*, 24, 67.
- Goldberg, D. E. (1989). *Genetic algorithms in search, optimization and machine learning*. New York: Addison-Wesley.
- Griffiths, J. F. (1995). Reduced kinetic models and their application to practical combustion systems. *Progress in Energy and Combustion Science*, 21, 25.
- Hindmarsh, A. C. (1983). In R. S. Stepleman, et al. (Ed.), *ODEPACK, A systematized collection of ODE solvers*. Scientific Computing. Amsterdam: North-Holland.
- Kee, R., Rupley, F., Meeks, E., & Miller, J. A. (1996). *CHEMKIN-III: A Fortran chemical kinetics package for the analysis of gas-phase chemical and plasma kinetics*. Sandia Report m SAND96-8216.
- Lam, S. H., & Goussis, D. A. (1994). The csp method for simplifying chemical kinetics. *International Journal of Chemical Kinetics*, 26, 461.
- Li, G., & Rabitz, H. (1997). Reduced kinetic equations of a co/h₂/air oxidation model by a special perturbation method. *Chemical Engineering Science*, 52, 4317.
- Lovas, T., Nilsson, D., & Mauss, F. (2000). Automatic reduction procedure for chemical mechanisms applied to premixed methane/air flames. *Proceedings of the Combustion Institute*, 28, 1809.
- Mass, U., & Pope, S. B. (1992). Simplifying chemical kinetics: Intrinsic low dimensional manifold in composition space. *Combustion and Flame*, 88, 239.
- Michalewicz, Z., & Schoenauer, M. (1996). Evolutionary algorithms for constrained parameter optimization problems. *Evolution and Computers*, 4, 1.
- Peters, N., & Williams, F. A. (1987). The asymptotic structure of methane-air flames. *Combustion and Flame*, 68, 185.
- Petzold, L., & Zu, W. (1997). *Model reduction for chemical kinetics: An optimization approach*. A.I.Ch.E. meeting, Los Angeles.
- Pope, S. B. (1982). An improved turbulent mixing model. *Combustion Science and Technology*, 28, 131.
- Pope, S. B. (1985). Pdf methods for turbulent reactive flows. *Progress in Energy and Combustion Science*, 11, 119.
- Pope, S. B. (1997). Computationally efficient implementation of combustion chemistry using in situ adaptive tabulation. *Combustion Theory Model*, 1, 41.
- Sirdeshpande, A. R., Ierapetritou, M. G., & Androulakis, I. P. (2001). Design of flexible reduced kinetic mechanism. *A.I.Ch.E. Journal*, 11, 2461.
- Tomlin, A. S., Turanyi, T., & Pilling, M. J. (1997). Mathematical methods for the construction, investigation and reduction of combustion mechanisms. In M. J. Pilling (Ed.), *Low-temperature combustion and auto ignition*, Chemical kinetics, Vol. 35. Amsterdam: Elsevier.
- Vajda, S., Valko, P., & Turanyi, T. (1985). Principal component analysis of kinetic models. *International Journal of Chemical Kinetics*, 17, 55.